AD-A043 384 NAVAL OCEAN SYSTEMS CENTER SAN DIEGO CALIF F/G 17/2.1
SIMULATION AND MEASUREMENT OF HIGH FREQUENCY IONOSPHERIC CHANNE--ETC(U)
APR 77 D B SAILORS, J R HILL

UNCLASSIFIED NOSC/TR-111 NL

1 OF 2
AD
A043 384

DATE FILMED
9-77
DDC

CONT.

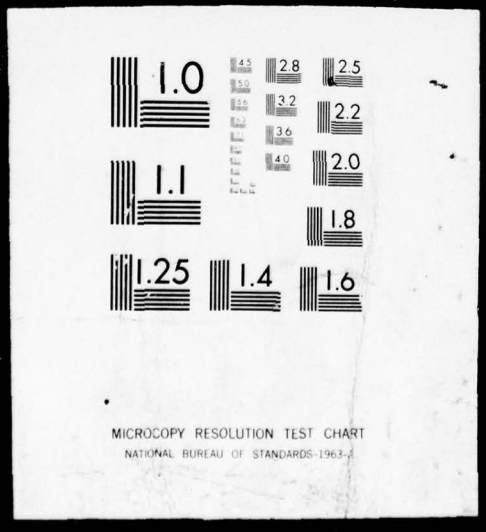

NOSC

NOSC / TR-111

NOSC / TR 111

Technical Report 111

SIMULATION AND MEASUREMENT OF HIGH FREQUENCY IONOSPHERIC CHANNELS

Time- and frequency-dispersive properties of hf sky wave propagation paths can be modeled for use in adapting signal format and signal processing algorithms for communication system development.

D.B. Sailors
J.R. Hill

22 April 1977

Interim Report for Period July 1976—September 1976

Prepared for
NAVAL ELECTRONIC SYSTEMS COMMAND
PME 107-031
Washington, DC 20360

Approved for public release; distribution is unlimited

NAVAL OCEAN SYSTEMS CENTER
SAN DIEGO, CALIFORNIA 92152

NAVAL OCEAN SYSTEMS CENTER, SAN DIEGO, CA 92152

AN ACTIVITY OF THE NAVAL MATERIAL COMMAND

RR GAVAZZI, CAPT, USN
Commander

HOWARD L BLOOD, PhD
Technical Director

ADMINISTRATIVE INFORMATION

Work was performed under 62721N, Task XF21222091 (NOSC B194B), by members of the Propagation Division. This interim report covers work from July through September 1976 and was approved for publication 22 April 1977.

The authors wish to express their indebtedness to CC Watterson of the Institute of Telecommunication Sciences (ITS), who sent copies of ITS reports on hf channel simulation and, in particular, to acknowledge that they relied heavily on the ITS report, Hf Channel-Simulator Measurements and Performance Analyses on the USC-10, ACQ-6, and MX-190 PSK Modems, by CC Watterson and CM Minister.

Released by
JH Richter, Head
Propagation Division

Under authority of
PC Fletcher, Head
Electromagnetic Systems Department

UNCLASSIFIED

SECURITY CLASSIFICATION OF THIS PAGE *(When Data Entered)*

REPORT DOCUMENTATION PAGE

READ INSTRUCTIONS BEFORE COMPLETING FORM

1. REPORT NUMBER: NOSC Technical Report 111 (TR 111)
2. GOVT ACCESSION NO.
3. RECIPIENT'S CATALOG NUMBER

4. TITLE *(and Subtitle)*: SIMULATION AND MEASUREMENT OF HIGH FREQUENCY IONOSPHERIC CHANNELS. Time- and frequency-dispersive properties of hf sky wave propagation paths can be modeled for use in adapting signal format and signal processing algorithms for communication system development.

5. TYPE OF REPORT & PERIOD COVERED: Interim – July 1976 – September 1976

6. PERFORMING ORG. REPORT NUMBER

7. AUTHOR(s): DB Sailors, JR Hill

8. CONTRACT OR GRANT NUMBER(s)

9. PERFORMING ORGANIZATION NAME AND ADDRESS: Naval Ocean Systems Center, San Diego, California 92152

10. PROGRAM ELEMENT, PROJECT, TASK AREA & WORK UNIT NUMBERS: 62721N, XF21222091 (NOSC B194B)

11. CONTROLLING OFFICE NAME AND ADDRESS: Naval Electronic Systems Command (PME 107-031)

12. REPORT DATE: 22 April 1977

13. NUMBER OF PAGES: 38

14. MONITORING AGENCY NAME & ADDRESS *(if different from Controlling Office)*

15. SECURITY CLASS. *(of this report)*: Unclassified

15a. DECLASSIFICATION/DOWNGRADING SCHEDULE

16. DISTRIBUTION STATEMENT *(of this Report)*

Approved for public release; distribution is unlimited.

17. DISTRIBUTION STATEMENT *(of the abstract entered in Block 20, if different from Report)*

18. SUPPLEMENTARY NOTES

19. KEY WORDS *(Continue on reverse side if necessary and identify by block number)*

Modems – high frequency
Simulation – radio reception
High frequencies – distortion
Ionograms
Ionospheric propagation – refraction
Wave dispersion – frequency and time

20. ABSTRACT *(Continue on reverse side if necessary and identify by block number)*

The report presents literature search of hf channel simulators, describes the Watterson model and its limitations, and discusses distortion of ionospherically propagated signals due to ionospheric refraction.

Significant dispersion occurs if the half-bandwidth exceeds $\pi / \sqrt{\Delta\tau / \Delta f}$, where $\Delta\tau / \Delta f$ (in s/Hz) is the ionogram slope at center frequency. For 100 kHz bandwidth, dispersion is significant if $\Delta\tau / \Delta f$ exceeds 3.14×10^{-4} ms/kHz, its measurement requiring 62.8 μs resolution.

Recommendations: For bandwidths above 2.5 kHz at night and 12 kHz during the day, add frequency dispersion correction filters to the Watterson simulator tap delay lines. To achieve required time delay resolution, use a complementary-sequence or modulated-pulse oblique sounder system. For the microprocessor or mini-

DD FORM 1 JAN 73 1473 EDITION OF 1 NOV 65 IS OBSOLETE S/N 0102 LF 014 6601

UNCLASSIFIED

SECURITY CLASSIFICATION OF THIS PAGE *(When Data Entered)*

Continuation of Block 20

computer controlled receiver, provide an atomic time-frequency standard and interfaces for terminal, CRT display, magnetic tape recorder, and auxiliary devices. When measuring modem performance capabilities with a channel simulator, take a "single and multiple distortions" approach. Use the Jones ray-tracing program to obtain the frequency dispersion relationships needed for applying corrective filters to the Watterson model; relate results to channel-caused system distortions. Use a suggested alternate approach if too many delay line taps would be needed.

OBJECTIVE

Establish a channel model and data base for designing sky wave modems. In particular, make a literature search of hf channel modeling and study both the Watterson model and the physics of the channel. Present a plan for acquiring available information to complete any necessary modification of the model.

RESULTS

1. There are two basic sources of distortion associated with hf paths: time dispersion and frequency dispersion.
2. The best known hf simulator is that developed at the Institute for Telecommunication Sciences by Watterson. It is limited to system bandwidths less than 2.5 kHz at night and less than 12 kHz during the day.
3. An important source of distortion of ionospherically propagated signals is the dispersion caused by ionospheric refraction.
4. For a 100 kHz bandwidth, dispersion caused by ionospheric refraction is significant if $\Delta\tau/\Delta f$ is greater than or equal to 3.14×10^{-4} ms/kHz.
5. To measure dispersion accurately enough to provide design information for dispersion correction filters, 62.8 μs resolution in time delay is necessary for a 100 kHz bandwidth.
6. An alternate approach is presented to hf channel simulation that is usable when the ionospheric dispersion is so large that it would call for an excessive number of taps in the Watterson model.

RECOMMENDATIONS

1. When using the Watterson hf channel simulator, install frequency dispersion correction filters on the tap delay lines for frequency bandwidths greater than 2.5 kHz at night and 12 kHz during the day.
2. To achieve the needed resolution in time delay, use an oblique sounder system employing complementary sequences or modulated pulses.
3. Control this sounder receiver by a microprocessor or a minicomputer.
4. Use atomic time or frequency standards for timing the frequency sweeps.
5. Use a processor that has interfaces for a terminal, a CRT display, a magnetic tape recorder, and an auxiliary device.
6. When measuring the performance capabilities of a modem with a channel simulator, use the single-and-multiple-distortions approach discussed in this report.
7. Use the Jones ionospheric ray tracing program to determine the time delay versus the frequency and range dispersion relationships to be used in the corrective filters.
8. Write a report discussing the significance of the various system distortions that can be caused by the channel. Relate these results to those obtainable from the Jones ray tracing program.

9. When the spread of arrival times of the ionospherically propagated signals causes an excessive number of taps to be required in the Watterson model, use the alternate approach to hf channel simulation, described in this report.

CONTENTS

ILLUSTRATIONS

TABLES

INTRODUCTION

Two methods are commonly used to evaluate the performance of hf radio communication systems: theoretical analyses and experimental measurements. Both are desirable and each has its advantages and limitations.

In theoretical analyses of system performance, various hf channel models have been used. Prediction techniques normally used are a form of non-real-time modeling or channel estimation and normally do not take account of the more transient propagation mechanisms.

Experimental measurements of system performance have been made over actual ionospheric links, but they are usually difficult to obtain and to apply. Most of the difficulties can be avoided by means of experimental measurements made with a stationary channel simulator in the laboratory. Consequently, there has been a rapidly growing interest in the development of hf channel simulators. (See bibliography entries under Watterson Model and all but the last two under Channel Modeling.)

An hf channel simulator provides a means for a communications engineer to optimize his use of an hf propagation path that has dispersive, time-varying properties. A simulator provides access to the values of parameters of an appropriate real-time ionospheric channel model which describes the path behavior adequately. "Real time" in this context implies that the parameter values can be updated at a rate exceeding the maximum significant rates of change of those parameters. Once the model has been developed, the engineer can then use it for optimally adapting the signal format and signal processing algorithms for communication system development.

In general, there are two basic sources of signal distortion associated with hf paths: time dispersion and frequency dispersion. The effects of these mechanisms can be represented by the "channel scattering function." This is a composite function that shows the dispersive effects of the path on an ideal impulse in the time domain and on a single cw tone in the frequency domain. Distinct propagation modes might be due to refraction in different ionospheric layers, multiple refractions in individual layers, or both. Any given scattering function is a valid description of the path behavior only for a specified rf carrier and only while the "dispersion surfaces," or probability distributions, remain sensibly constant. In the longer term, time variations of the path parameters will cause changes in the number of modes, the mode amplitudes and delays, and the shape of the distributions associated with each of the modes.

Although an unproven channel model can provide useful information, results must be weighed with caution since they may not be typical of the hf medium. More useful would be a mathematically tractable channel model that is known to be a valid representation of the hf medium for the largest practicable percentage of typical hf links. On economic grounds, it is important for the channel modeling techniques employed to be no more complex than necessary and to be tailored to provide only that information which has direct relevance to the communicator. As an example, the modeling detail needed for wide band systems is greater than that needed for narrow band systems because of the added frequency dispersion in the ionosphere. For narrow band systems less detail would be necessary.

SYSTEM DISTORTIONS

In any digital radio communication system, the signal delivered to the modem receiver is generally a distorted version of the signal that the modem transmitter should ideally generate.[1] The sources of distortion in a digital radio communications system are as follows:

Transmitting Equipment

- Modem transmitter
- Rf transmitter

Channel (transmitting to receiving antenna)

Receiving equipment

- Rf receiver
- Modem receiver

The types of transmitting and receiving equipment distortion that can occur are as follows:

Additive

- Thermal noise
- Quantizing noise
- Interference (internal)

Multiplicative

- Synchronization (delay)
- Filtering (frequency selective)
- AGC (time selective)

Nonlinear

The types of distortion that a radio channel can impose on a signal are as follows:

Additive

- Gaussian noise
- Atmospheric noise
- Manmade noise
- Interference (unwanted signals)

Multiplicative

- Multipath time scatter (frequency selective)
- Dispersion time scatter (frequency selective)
- Doppler frequency scatter (time selective)
- Fading frequency scatter (time selective)

---

[1] Office of Telecommunications Report 75-56, HF Channel-Simulator Measurements and Performance Analyses on the USC-10, ACQ-6, and MX-190 PSK Modems, by CC Watterson and CM Minister, July 1975

All these types of channel distortion are present on ionospheric communication channels. Dispersion is a variation in the velocity of propagation with frequency over any path in a channel. It causes the delay characteristics for that path to vary with frequency.

In general, the small distortions introduced by the transmitting equipment are relatively unimportant and can be ignored. The channel distortions, however, can be substantial and are of primary importance. While the distortions introduced by the receiving equipment may not be larger than the distortions introduced by the transmitting equipment, their effects on the system performance are much greater when multiplicative distortion is present in the channel, and their presence cannot be ignored.

WATTERSON CHANNEL SIMULATOR

Watterson et al., of the Institute for Telecommunication Sciences (ITS), undertook a program in 1965 to develop specialized propagation measuring equipment, to obtain measurements of typical ionospheric channels, and to analyze those measurements to determine the validity and bandwidth limitations of a proposed channel model. Based on these measurements, an ITS ionospheric channel simulator was built.[2,3,4] This simulator is presently capable of accurately simulating all types of channel distortion listed except manmade noise. They found that their channel model could be considered valid over a bandwidth that is approximately one-fourth of the reciprocal of the effective time spreads on the ionospheric paths. For the measured channels, these bandwidths were 2.5 kHz for the nighttime sample to a maximum of 12 kHz for the daytime samples. They feel that if the time spreading on each measured nighttime path were caused primarily by the differential propagation time between the two magnetic components, the use of separate taps for each magnetoionic component would yield a model that would be valid over a larger bandwidth.

A block diagram of the channel simulator as it is used in non-space-diversity measurements is presented in figure 1. The input (transmitted) signal feeds a delay line with several taps, one for each propagation mode or path, numbered 1,2, . . . n, where n is the maximum number of modes or paths. The present Watterson simulator shown in figure 1 has four taps. The position of each tap can be independently adjusted to a delay, τ_i. This adjustment sets the differential path delays and determines the multipath distortions. Each tap delivers a delayed but effectively undistorted version of the transmitted signal to a path gain multiplier, where the signal is modulated in amplitude and phase by an independent, stationary, complex, baseband function termed the path gain function, $G_i(t)$, to provide the frequency-scatter distortion (both Doppler and fading) on that path. Each path gain function

$$G_i(t) = [\bar{G}_i + \tilde{G}_i(t)] \exp(j2\pi\nu_i t), \quad (1)$$

---

[2]CC Watterson, JR Juroshek, and WD Bensema, Experimental Confirmation of an Hf Channel Model, IEEE Trans Commun Technol, v 18, p 792-803, December 1970

[3]ESSA Technical Report ERL 112-ITS 80, Experimental Verification of an Ionospheric Channel Model, by CC Watterson, JR Juroshek, and WD Bensema, July 1969

[4]ESSA Technical Report ERL 127-ITS 89, Recommended Specifications for Ionospheric Channel and Atmospheric Noise Simulators, by CC Watterson and RM Coon, September 1969

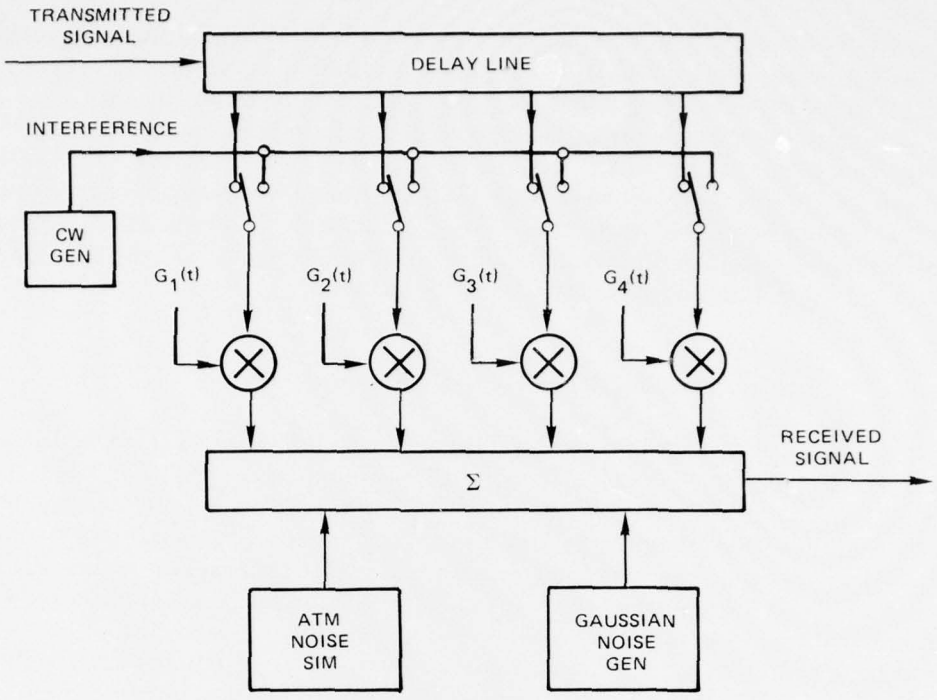

Figure 1. Channel simulator for non-space-diversity measurements.[1]

where $\bar{G}_i$ is a complex nonfading specular component and $\tilde{G}_i(t)$ is a complex fading Gaussian-scatter component with Rayleigh amplitude distribution and uniform phase distribution. The exponential factor introduces a Doppler frequency shift, ν_i, that is common to the specular and Gaussian-scatter components.

The spectral characteristics of each path gain function, $G_i(t)$, are described by the path gain spectrum, $V_i(\nu)$, as follows:

$$V_i(\nu) = \frac{1}{\bar{a}_i}\ \delta(\nu - \nu_i) + \frac{1}{\sqrt{2\pi}\sigma_i\tilde{a}_i}\ e^{-(\nu - \nu_i)^2/2\sigma_i^2}, \qquad (2)$$

which is the power spectrum of $G_i(t)$. The first term is the specular component, with a Dirac-delta function spectrum and specular attenuation $\bar{a}_i$; while the second term is the Gaussian-scatter component, which has a Gaussian-shaped spectrum with a frequency spread (fading rate) σ_i and a Gaussian-scatter attenuation $\tilde{a}_i$. The specular and Gaussian-scatter attenuations are both power ratios: the transmitted signal power divided by the received power in that component. Equation (2) is illustrated in figure 2. Five parameters together completely specify each path gain function and path gain spectrum: specular component attenuation, specular component phase, Gaussian-scatter component attenuation, Gaussian-scatter component frequency spread, and Doppler shift.

The delayed and modulated signals from the four paths in figure 1 are summed with each other and with Gaussian or simulated atmospheric noise to form the output (received) signal. When internally supplied cw interference or other externally supplied interference is used, it is introduced in place of one or more of the delayed signals so that independent Doppler and fading can be introduced. If wide band externally supplied interference is used,

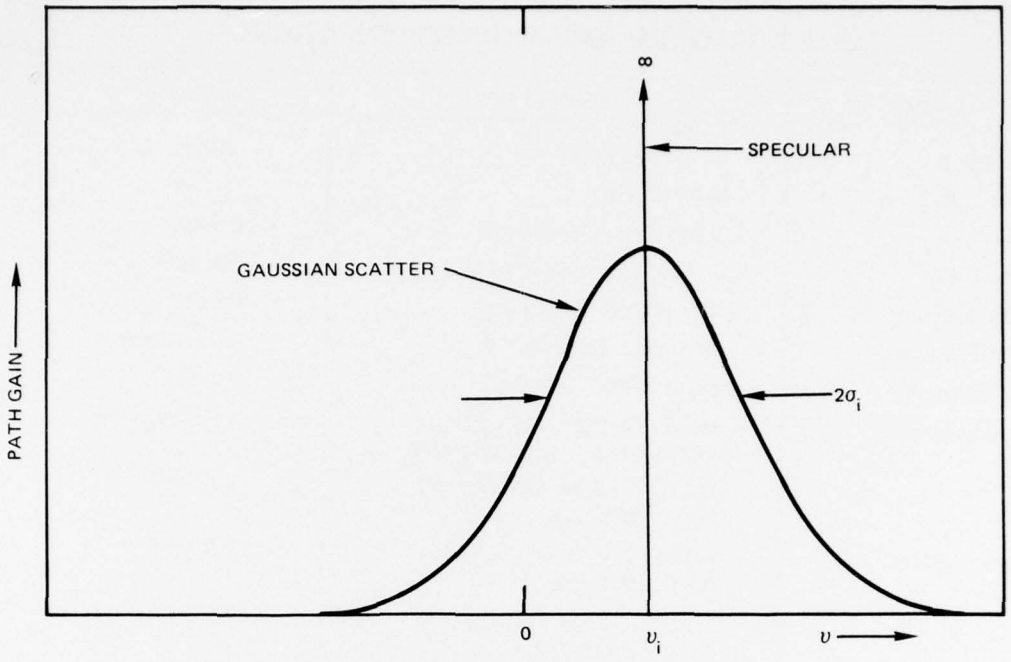

Figure 2. Path gain spectrum.[1]

a second delay line is necessary for the interference, and this is not presently available. (Wide band here means having a bandwidth larger than the reciprocal of the maximum differential delay typical of hf.)

In hf channel simulation, each Gaussian-scatter component, $G_i(t)$, represents in general one magnetoionic component when the two magnetoionic components in a high or low ray have significantly different Doppler shifts or delays. When the Doppler shifts and delays are essentially the same, a single path can represent both components.

The channel simulator also has linear dispersion filters that can be inserted in any path between the delay-line tap and the path gain multiplier. They are all-pass filters with delay characteristics that are linear in frequency and with selectable amounts of dispersion (delay slope). Since the filters were developed for vlf/lf simulation, they do not necessarily represent the time-delay-frequency slope of an oblique ionogram and are not usable for hf simulation.

Table 1 summarizes the numerical values of the channel simulator parameters that are available in the ITS Ionospheric Channel Simulator. The decibel path attenuations, A_i, are defined as 10 log (a_i). The attenuation values shown are accurate over the range of attenuations normally used except where $A_i \rightarrow \infty$. Here, 99 dB settings are used, and accuracy is of no practical importance.

TABLE 1. CHANNEL SIMULATOR SPECIFICATIONS.[1]

Parameter	Available Values	Accuracy
Bandwidth, B	3, 6, or 12 kHz	– –
Number of Paths, n	4 maximum	– –
Delay, τ_i	0 to 10 ms in 20-μs steps	0.5 μs
Dispersion, D_i	0, 100, 220, and 320 μs/kHz	2 X 10^{-2}
Specular Atten, $\bar{A}_i$	0 to 100 dB continuous	0.2 dB*
Specular Phase, $\bar{\theta}_i$	continuous (modulo 2π)	0.01 radians
Scatter Atten, $\tilde{A}_i$	0 to 100 dB continuous	0.2 dB*
Frequency Shift, ν_i	Intl Synthesizer: 0, ±1, ±2, or ±5 X 0.01, 0.1, 1, 10, or 100 Hz	1 X 10^{-4}
	Ext Synthesizer: -500 to +500 Hz in 1-mHz steps	1 X 10^{-6}
Frequency Spread, $2\sigma_i$	Each Path: 1, 2, or 5 X 0.01, 0.1, 1, 10, or 100 Hz	2 X 10^{-2}
	One Path: 1.00, 1.33, 1.78, 2.37, 3.16, 4.22, 5.67, or 7.50 X 0.01, 0.1, 1, 10, or 100 Hz	2 X 10^{-2}
Fading Spectrum, $v_i(\nu)$	3-pole approximation of Gaussian	<0.03 dB**
Signal to Noise, E_b/N_d	-100 to +90 dB continuous,	
	Gaussian	0.2 dB*
	Atm	0.5 dB*
Atmospheric Noise Impulsiveness, V_d	hf: 7.2 dB in 2.7 kHz	– –
	lf: 10.8 dB in 2.7 kHz	– –
	lf: 9.0 dB in 2.7 kHz	– –
Signal to Interference, S/I	-100 to +90 dB continuous	0.2 dB*
Space Diversity	Single or independent dual	– –
Internal Distortions		
Additive	<-70 dB relative to signal + noise	– –
Nonlinear	<-70 dB relative to signal + noise	– –

*Over range of significance

**Theoretical

CHANNEL CHARACTERIZATION

In analyzing the performance capabilities of modems suffering multiplicative channel distortions, it is useful to have theoretical statistical descriptions of the channel frequency-scatter and time-scatter characteristics in addition to the channel simulator parameters. Two statistical descriptions for stationary time-varying channels given by Bello[5] and others are the channel correlation function and the channel scatter function, which can be obtained from the channel time-varying frequency response. From figure 1 and equation (1), it can be seen that the complex channel time-varying frequency response for the ITS channel simulator model

$$H(f,t) = \sum_{i=1}^{n} G_i(t) \exp(-j2\pi\tau_i f) \tag{3}$$

and the channel correlation function

$$R(\Delta f,\Delta t) = \lim_{t_1\to\infty} \frac{1}{2t_1} \int_{-t_1}^{t_1} H^*(f,t)H(f+\Delta f, t+\Delta t)\, dt \quad , \tag{4}$$

where the asterisk (*) denotes a complex conjugate. The channel scatter function then is the double Fourier transform of R ($\Delta f,\Delta t$):

$$S(\tau, \nu) = \int_{-\infty}^{\infty} \int_{-\infty}^{\infty} R(\Delta f,\Delta t) \exp(j2\pi\tau\Delta f - 2\pi\tau\Delta t)\, d\Delta f d\Delta t. \tag{5}$$

For the ITS channel simulator model, it can be shown that the channel scatter function

$$S(\tau,\nu) = \sum_{i=1}^{n} \delta(\tau - \tau_i)\, V_i(\nu) \quad , \tag{6}$$

where $V_i(\nu)$ is the path gain spectrum specified by equation (2). While $S(\tau,\nu)$ is dimensionless, it is a power-ratio density function: it specifies the power in the received signal per unit delay and per unit frequency offset, divided by the transmitted power, as a function of delay, τ, and frequency offset, ν. It specifies how the signal is scattered or distributed in time by the multipath delays and in frequency by the Doppler shifts and fading. It is not a description of a signal, but rather what the channel does to a signal.

Additional statistical descriptions are also useful (Watterson, et al)[3]. The channel frequency-scatter function

$$V_c(\nu) = \int_{-\infty}^{\infty} S(\tau,\nu)\, d\tau$$

$$= \sum_{i=1}^{n} V_i(\nu) \quad . \tag{7}$$

[5]PA Bello, Characterization of Randomly Time-Variant Linear Channels, IEEE Trans Commun Syst, v 11, p 360-393, December 1963

The channel frequency-scatter function, like the path gain spectrum of each path, can be described in terms of a Doppler shift and frequency spread. To do this, it is necessary to normalize equation (7) so that its integral is unity. Since $S(\tau,\nu)$ is a power-ratio density function, it follows that the channel attenuation

$$a_c = \frac{1}{\int_{-\infty}^{\infty}\int_{-\infty}^{\infty} S(\tau,\nu)\, d\tau d\nu} \tag{8}$$

and the normalized channel frequency-scatter function is $a_c V_c(\nu)$. The channel Doppler shift then is the first moment of the normalized channel frequency-scatter function:

$$\nu_c = \int_{-\infty}^{\infty} \nu[a_c V_c(\nu)]\, d\nu$$

$$= a_c \sum_{i=1}^{n} \left(\frac{1}{\bar{a}_i} + \frac{1}{\tilde{a}_i}\right) \nu_i \quad , \tag{9}$$

where equation (2) and equation (7) were used to obtain the last form. The channel frequency spread, $2\sigma_c$, is defined as twice the square root of the second central moment of the normalized channel frequency-scatter function:

$$2\sigma_c = 2\left[\int_{-\infty}^{\infty} \nu^2\, [a_c V_c(\nu - \nu_c)]\, d\nu\right]^{1/2}$$

$$= 2\left[a_c \sum_{i=1}^{n} \left(\frac{\nu_i^2}{\bar{a}_i} + \frac{\nu_i^2 + \sigma_i^2}{\tilde{a}_i}\right) - \nu_c\right]^{1/2} . \tag{10}$$

These definitions of channel Doppler shift and channel frequency spread are consistent with the corresponding path definitions; ie for a single path channel, equations (9) and (10) yield the path Doppler shift and path frequency-spread values of equations (1) and (2).

The time-scatter characteristics of the channel can be described in a similar way. The channel time-scatter function

$$U_c(\tau) = \int_{-\infty}^{\infty} S(\tau,\nu) d\nu$$

$$= \sum_{i=1}^{n} \left(\frac{1}{\bar{a}_i} + \frac{1}{\tilde{a}_i}\right) \delta(\tau - \tau_i) \quad . \tag{11}$$

The channel delay, τ_c, is the first moment of the normalized channel time-scatter function:

$$\tau_c = \int_{-\infty}^{\infty} \tau [a_c U_c(\tau)] \, d\tau$$

$$= a_c \sum_{i=1}^{n} \left(\frac{1}{\bar{a}_i} + \frac{1}{\tilde{a}_i} \right) \tau_i , \qquad (12)$$

and the channel time spread, $2\rho_c$, is twice the square root of the second central moment of the normalized channel time-scatter function:

$$2\rho_c = 2 \left[\int_{-\infty}^{\infty} \tau^2 [a_c U_c(\tau - \tau_c)] \, d\tau \right]^{1/2}$$

$$= \left[a_c \sum_{i=1}^{n} \left(\frac{1}{\bar{a}_i} + \frac{1}{\tilde{a}_i} \right) \tau_i^2 - \tau_c^2 \right]^{1/2} . \qquad (13)$$

If time in the preceding equations, (1) through (13), is measured relative to the transmitter timing, all path delays, τ_i, are positive, and the channel time delay is usually much larger than the channel time spread. Since a constant time delay can be subtracted from the channel (ie, the same constant subtracted from all path delays) without changing the distortion present on the signal, it is convenient in analyzing modem-receiver performances to measure time such that the channel delay in equation (12) is zero. When this is done, the channel scatter function in equation (6) for a channel with two Gaussian-scatter paths (no specular components) would appear in general as shown in figure 3. The two paths might represent one- and two-hop propagation modes via the F layer of the ionosphere. Because the channel time delay was set to zero, the first path has a negative delay τ_1 and the second path has a positive delay τ_2.

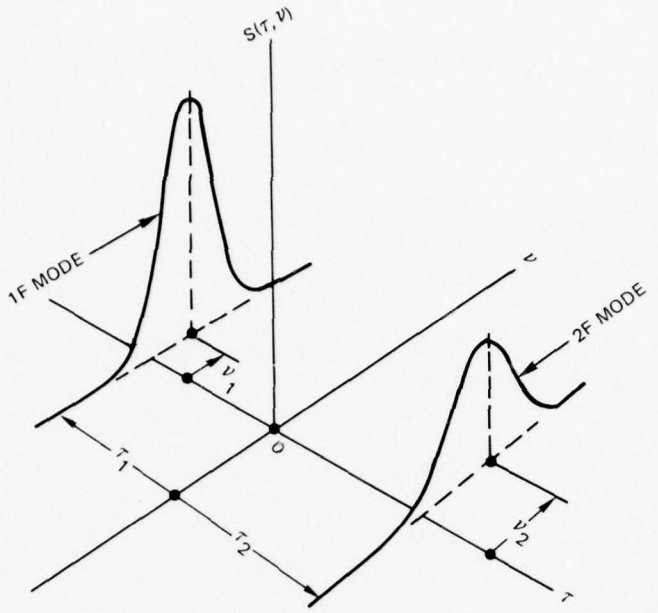

Figure 3. Scatter function for a two-path channel.

DISPERSION DUE TO IONOSPHERIC REFRACTION

A source of distortion of ionospherically propagated signals is the dispersion as a consequence of ionospheric refraction. This dispersion manifests itself by altering the phases of the various frequency components of a signal so that they are not coherently combined by the correlator.[6,7,8]

The phase distortion imposed on a signal by ionospheric dispersion may be represented by a transfer function of the form $e^{-i\phi(f)}$ where the argument $\phi(f)$ represents the variation with frequency of the phase retardation over the propagation path. If $\phi(f)$ is a linear function of f, there is no dispersion, and the transfer function then represents only the propagation delay over the path. Such a group delay, τ, may be represented as

$$\tau = \frac{d\phi(f)}{df}, \text{ a constant.} \tag{14}$$

However, if the variation of ϕ with frequency is nonlinear, so that

$$\tau = \frac{d\phi(f)}{df}, \text{ not a constant,} \tag{15}$$

then dispersion, with its consequent distortion, is present.

---

[6]Electrophysics Laboratories Project Report 236, Dispersion Correction Study, by RN DeWitt, JR Earhart, and JD Kolesar, August 1973

[7]Electrophysics Laboratories Project Report 243, Dispersion Correction Study, by RN DeWitt, JL Wheeler, and FJ Woods Jr, March 1974

[8]Electrophysics Laboratories Project Report 207, Estimates of Distortion of a Wideband Signal Propagated via the Ionosphere, by RN DeWitt, JR Earhart, and JD Kolesar, September 1972

In the development of the Watterson tap delay simulation mode, it was assumed that the time delay was stationary with frequency. Watterson himself found that his model was limited to a bandwidth of 12 kHz for daytime samples and 2.5 kHz for nighttime samples. If this model is to be used for larger bandwidths, it must incorporate some means for tolerating or adapting to the existing ionospheric phase shift and delay.

An examination of ionospheric sounding seems to indicate that the group retardation over the path varies smoothly with the portion of the hf spectrum where any given propagation mode exists. For a fixed path, the group delay distortion may be different for each mode. If such is the case, corrective filters could be added to each tap or precorrection of the signal could be feasible. The amount of dispersion on a signal is a function of the particular ray paths between the terminals of the communication link. Consequently, the dispersion will vary as the path end points vary, and a correction made for a signal between the fixed terminal and a remote point is not appropriate to a path between the fixed terminal and another point sufficiently displaced from the first.

In propagating via the ionosphere, if the signal experiences a frequency dependent phase delay $\phi(f)$, we may approximate $\phi(f)$ by a Taylor series expansion about the band center, f_o. Thus

$$\phi(f) = \phi(f_o) + \phi'_o(f_o)(f - f_o) + 1/2\,\phi''_o(f_o)(f - f_o)^2 + \ldots . \tag{16}$$

We ignore the first two terms, since the Watterson model includes these terms in equation (3). Assuming that the third term well represents the remaining variation of phase, the variation may be regarded as seriously degrading to the signal if, over the interval extending from the band center to the band edge – a difference of b/2 in frequency –, the phase contribution of the third term varies through a half-cycle. That is, if

$$1/2\left[\phi''_o(f_o)(b/2)^2\right] = \pi/2 . \tag{17}$$

Solving for $\phi'_o(f_o)$, we find that this condition occurs if

$$\phi''_o(f_o) = \frac{d\tau}{df} = \frac{4\pi}{b^2} . \tag{18}$$

The dispersion may be regarded as significant if $b/2 \geq \frac{\pi}{\sqrt{\Delta\tau/\Delta f}}$, where $\Delta\tau/\Delta f$ in s/Hz is the slope on the ionogram at f_o, the center frequency. If the spectral components are summed without correction under such circumstances, the components of the signal at band center will tend to be canceled by the frequency components of the signal at band edge. Intermediate components will be only partially canceled; thus the condition does not imply a strong degradation of the signal. Rather it represents the point at which dispersion begins to become serious. Figure 4 is a plot of b/2 in kHz equal to $\frac{\pi}{\sqrt{\Delta\tau/\Delta f}}$, where $\Delta\tau/\Delta f$ is in ms/kHz. If the dispersion has been corrected, figure 4 is a measure of the resolution necessary to obtain adequate dispersion data for simulation purposes. At b/2 of 50 kHz, for instance, the resolution necessary would be 62.8 μs in time delay.

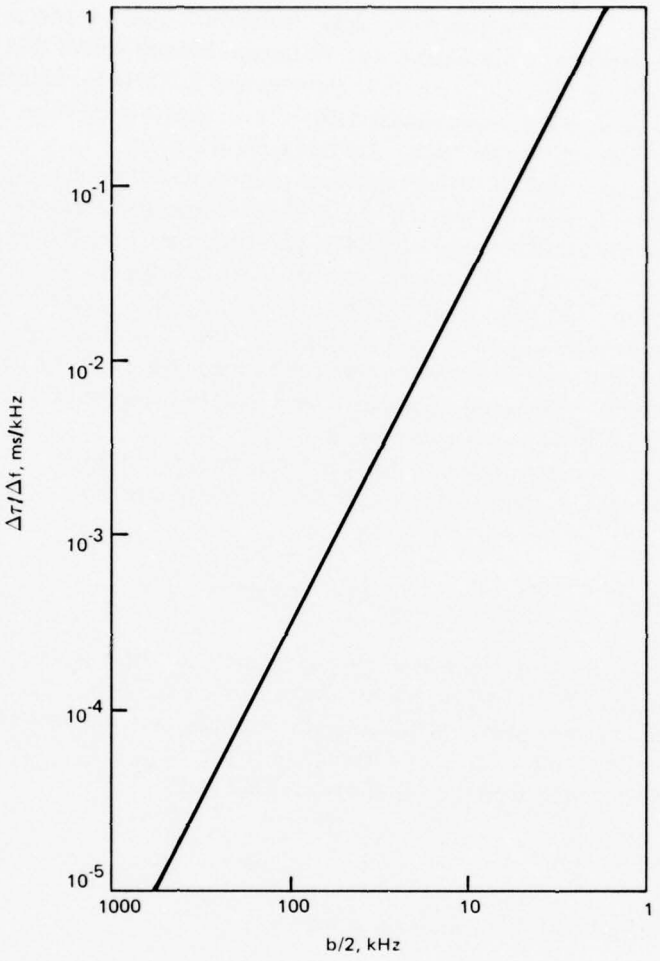

Figure 4. Ionospheric bandwidth dispersion limit.

Figure 5 is a backscatter ionogram from the Chapel Bell Radar at Whitehouse, Virginia.[6] The slope at the frequency of measurement was 5×10^{-5} ms/kHz. This corresponds to a distortion half-band, using the above criteria, of 260 kHz. Straight lines are drawn tangent to the oblique ionogram traces at the frequency of measurement, for two targets. A line parallel to the upper trace is drawn so as to intersect the lower, and the difference in slopes of the lines is determined from a measurement of their separation at a distance from their intersection corresponding to 3 MHz. This difference divided by the time separation of the two ionogram traces at the frequency of measurement gives the range dependence of dispersion.

At the MUF of any of the received modes $d\tau/df = \infty$. If the upper edge of the bandwidth b is at the MUF, a worst case for dispersion is established. The boundary condition defined by the MUF can be used near the MUF to define a power series fit to the ionogram

$$\tau = \sum_{j=1}^{n+1} A_j (f - f_o)^{j-1}, \tag{19}$$

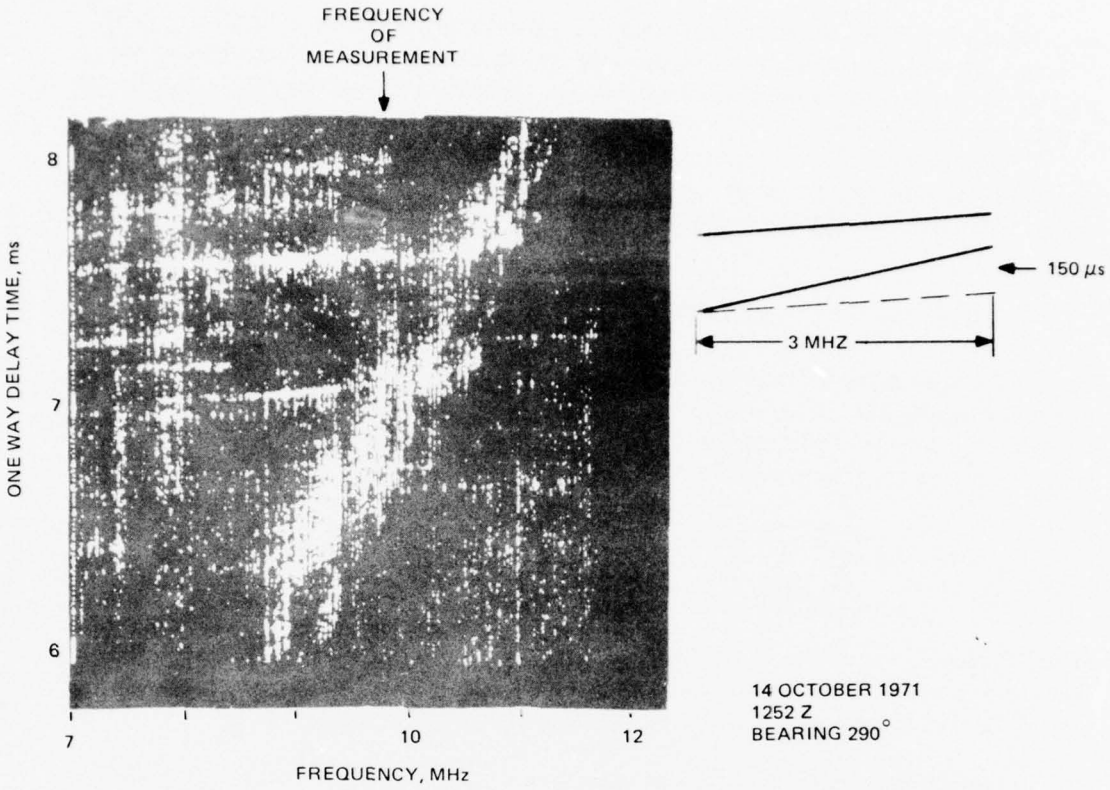

Figure 5. Backscatter ionogram from Whitehouse VA, scaled to determine the range dependence of dispersion (10/14/71, 1252Z).[6]
Note: A backscatter ionogram shows reflections for several ranges; whereas an oblique incidence ionogram is for only one range. Each range has a different slope.

where

τ = delay time (ms)

f_o = carrier frequency (MHz)

f = operating frequency (MHz)

n = order of polynomial

A_j = power series coefficients.

For the power series model, the phase distortion

$$\Delta\phi_1 = \sum_{j=3}^{n+2} \left[A_{j-1}(f-f_o)^{j-1}\right]/(j-1)\,. \tag{20}$$

It is awkward to work with a power series expansion in this respect because an adjustment of the coefficient of a higher term to improve the fit will affect the correctness of any

prior adjustment of lower order coefficients. To avoid this interaction, it is preferable to employ a set of orthogonal functions, the adjustments for which are independent of one another.[6] Orthogonalization of simple power laws over the bandwidth of the signals lends to phase-correcting functions which are Legendre polynomials.[6]

The amount of dispersion appearing on the oblique ionogram varies with time of day, path range, season, and mode as well as with environmental conditions. Usually the slope will be larger at night than during the day and at short ranges.

EXTENSION OF SIMULATION TECHNIQUE TO WIDE BANDWIDTHS

The time delay for each mode or propagating path is a measurable quantity over the frequency bandwidth. If we assume that the time delays for the i^{th} mode are known as a function of frequency and range, then the time delay can be approximated by a polynomial function of frequency and range:

$$\tau_i (f_o, R_o) = \sum_{n=1}^{n+1} \sum_{j=1}^{j+1} A_{nj} (f - f_o)^{n-1} (R - R_o)^{j-1}, \qquad (21)$$

where f_o and R_o are reference frequency and range. The coefficients can be determined from measurements or from ionospheric ray tracing.[9]

Having determined $\tau(f,t)$, then a new $G_i(t,f)$ is found by using the relationship

$$G_i(t,f) = g_i(t) + g_i'(f) . \qquad (22)$$

Equation (22) includes $g_i(t)$, which is the $G_i(t)$ of the Watterson model.

The function of $g_i'(f)$ can be applied by adding a corrective filter to each tap which would represent the dispersion spectra, $g_i'(f)$, relative to f_o, the bandwidth center. Each f_o would have a different filter. The number of taps would depend on the amount of correction desired for each filter and would be equal to the $b\Delta T$ product of the ionospherically distorted signal, where b is the bandwidth and ΔT is the range of times over which the various modes are spread.

Typically, the spread of arrival times might be a few milliseconds, so for a 100 kHz signal a few hundred taps would be required. One could also model the various modes individually, with fewer taps. For example, if the F-scan of the path indicates a mode has a range of delay of ΔT over the bandwidth of interest, W, one may be able to make a satisfactory signal mode model with $W\Delta T$ taps. However, it may prove to be awkward to orchestrate several separate modes in this fashion.

---

[9] Office of Telecommunications Report 75-76, A Versatile Three-Dimensional Ray Tracing Computer Program for Radio Waves in the Ionosphere, by RM Jones and JJ Stephenson, October 1975. This is a versatile program for tracing rays through an anisotropic medium whose index of refraction varies continuously in three dimensions. The program can represent the refractive index by either the Appleton-Hartree or the Sen-Wyller formula. The program has nine ionospheric models for electron density, eight perturbations (irregularities) to the electron density models, four models of the earth's magnetic field, and four models of the electron collision frequency.

For a real-time model, tapped delay lines as discussed above might be well suited to the task. The necessary tap weights could be computed fast enough in a small processor to keep them suitably updated for modeling gradual ionospheric variations, while the ionospheric "filter" would take place in the time domain and could take place at a much higher rate. A similar process could be used to correct distortion in a working system.

AN ALTERNATE APPROACH TO HF CHANNEL SIMULATION

RN DeWitt[10] has expressed some reservations about the Watterson channel simulator. These mostly concern his use of tap weights that are "complex (bivariate) – Gaussian stationary ergodic random processes" with zero mean. DeWitt feels that this kind of modeling seems to be more of a carryover from early low resolution studies. That is, ionospheric signals have always been observed to undergo a great deal of fluctuation as a result of unresolved multiple propagation modes that interfere with one another.

However, there is some question as to whether these same fluctuations would appear on a single resolved mode. For the modes to be entirely resolved, a rather wide bandwidth would be required, particularly in the case of magnetoionic splitting. But once the modes are resolved, what mechanisms exist to produce fluctuations? Of course, there are some. For example, there are absorption effects, such as SIDs, that will reduce signal strength, and TIDs, which may either increase or decrease signal strength of a given mode through focusing. Diffraction by sporadic E irregularities could constitute a third mechanism. These phenomena are not always present, however, and even when they are, it is unlikely that they are well modeled by a bivariate Gaussian zero mean process. Diffraction from irregularities is the one that could sometimes produce a Gaussian process.

An alternate approach to hf channel simulation is presented here. This approach provides the transfer function for a single propagation mode; the effects of multimoding would have to be handled by a superposition of such transfer functions. A subset of a receiver system has been described. The character decoding can be done many other ways but has been included here to illustrate the use of the ionospheric model applied to both a random waveform and a pure character waveform.

A waveform, W(t), can be written as a modulation function, M(t), and a carrier wave, $\cos(2\pi f_c t + \phi_c)$:

$$W(t) = M(t) \cos(2\pi f_c t + \phi_c) . \tag{23}$$

The frequency independent portion of the function $G_i(t,f)$ can be included in the model when each sample W(t) is calculated. Thus

$$W_i(t + g_i(t)) = M(t + g_i(t)) \cos(2\pi f_c (t + g_i(t)) + \phi_c) , \tag{24}$$

---

[10] International Telephone and Telegraph Avionics Division Electro-Physics Laboratories Letter serial no. RD-8386, by RN DeWitt, to Naval Electronics Laboratory Center (DB Sailors), Subject: Review of Watterson's IEEE paper, 30 September 1976

where $g_i(t)$ is a random function having the desired characteristics, eg Gaussian, nonstationary, etc. The $\tau_i(f)$ portion of G_i is folded into the model after taking the fast Fourier transform (FFT) of $W_i(t)$. The spectrum of the final waveform W'(t)

$$\mathrm{FFT}[W'(t)] = \mathrm{FFT}[W(t + g_i)]\, e^{-2\pi j \int_0^f \tau_i(\nu)d\nu} . \tag{25}$$

Note that if τ is represented by a polynomial in f as in (21), then the exponential in (25) and (3) is a phase shift

$$\phi_i'(f) = \phi_i(f) - 2\pi f(a_i + b_i f/2 + c_i f^2/3 + \ldots) . \tag{26}$$

DECODING THE CHARACTER FROM THE SPECTRUM

Correlations can be calculated very rapidly in the frequency domain. We are nearly through at this point, since we already have the FFT of W'. By using precalculated stored spectra of the character set we have immediately the correlation function S_ℓ of the ℓ^{th} character:

$$\mathrm{FFT}[S_\ell(t)] = \mathrm{FFT}[C'(t)] \times \mathrm{FFT}[W'(t)] . \tag{27}$$

The function $S_\ell(t)$ will peak above the threshold at a value of t corresponding to the position of the character in the original wave.

SPECTRA OF THE CHARACTER SET

The spectrum of each character, FFT[C'(t)], is calculated by using the same process as that of W'(t). That is, each of the modes included in the calculation of W' uses the time delays τ. The only difference between C'(t) and W'(t) is that $g_i(t)$ is set to zero for calculating C'(t). This is because the mean time delay (nonrandom part) is accounted for in τ. Thus the FFT(C') can be precalculated when $\tau_i(f)$ is measured.

SAMPLING CONSIDERATION

Assume that a signal with bandwidth, B, is processed in a linear filter. No signals higher in frequency than $f_c + B$ nor lower than $f_c - B$ will be produced. If B = 100 kHz, the sampling rate must be at least once every 5 seconds if the Nyquist frequency, f_N, is to equal B. 1024 samples will cover about 5 ms, which should be enough for forward and inverse transforms to be calculated in real time. The resulting frequency resolution is 200 Hz.

ALIASING

The carrier frequency can be "shifted" to zero frequency provided that the Nyquist frequency (sampling interval) is related to the carrier frequency as follows:

$$f_c = 4mf_N, \text{ where m is an integer.} \tag{28}$$

The transform will be shifted in frequency so that $f' = f - f_c$.

$$\begin{aligned} -f_N &\leftarrow f_c - f_N \\ 0 &\leftarrow f_c \\ +f_N &\leftarrow f_c + f_N \end{aligned} \tag{29}$$

The requirement here is that the incoming waveform is band-limited to plus and minus B.

VERIFICATION OF THE CHANNEL MODEL

Preferably, both for theoretical analyses and as the basis for simulator designs, a desirable channel model would be one that is known to be a valid representation of the hf medium for the largest practicable percentage of typical hf links. Some of the detailed characteristics of the ionosphere needed to specify such a model may not have been measured.

In 1969 Watterson reported experimental verification of his ionospheric channel model.[2,3] A hybrid time-and-frequency domain method was used to obtain propagation measurements. In the transmitter, an accurate cesium-beam frequency standard was used to generate a carrier that was amplitude modulated to obtain coherent pulses with near-Gaussian envelopes of 50 μs duration at a 200-Hz rate. The same reference was used to generate 11 cw signals (tones) of equal amplitude at frequencies that coincided with 11 spectral components of the pulses. The transmitter output (both the power spectrum and the time function) is illustrated in figure 6. The 11 tones were symmetrically spaced in a 9.6 kHz band about the carrier frequency, f_o. The low level composite signal was amplified linearly to 5 kW. In the receiver, each of the 11 tones (with delays and modulation imposed by the ionospheric channel) was separated and heterodyned to a second IF of 80 Hz. The received signal was also passed through an 11-notch filter that removed the 11 tones, and the resulting pulses were envelope detected and compared against a 200 Hz reference to obtain measurements of τ_i. The 80 Hz IF tones were FM recorded on an analog tape recorder with an 80 Hz reference signal. During playback, the reference signals were used to detect each of the 11 IF tones to obtain the real and imaginary components of the time-varying frequency responses of the measured channel, $H_m(f_k,t)$, at the 11 values of f_k.

Propagation measurements were made over a 1294 km link between Long Branch, Illinois and Boulder, Colorado. Nighttime measurements were made at 5.86 MHz and daytime measurements at 9.259 MHz, both far enough below the predicted MUF that both one- and two-hop modes probably would be seen. About 7 hours of recorded nighttime measurements and 10 hours of daytime measurements were obtained during three periods in November 1967. Times were avoided near sunrise and sunset, when propagation conditions were

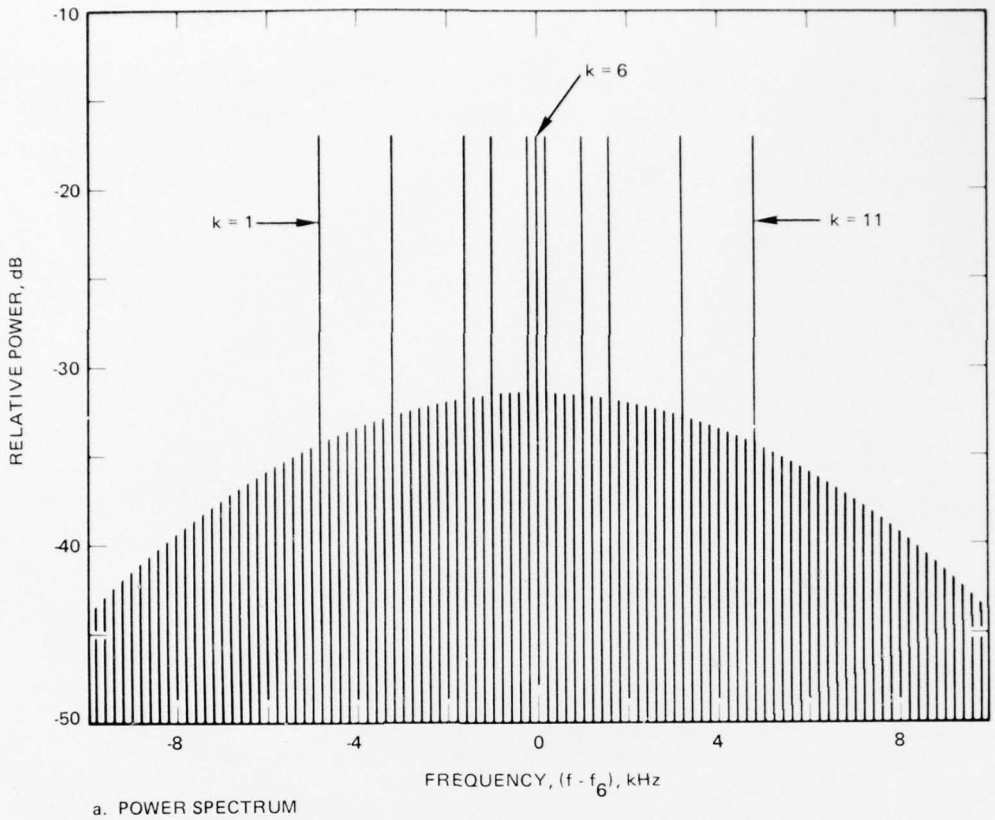

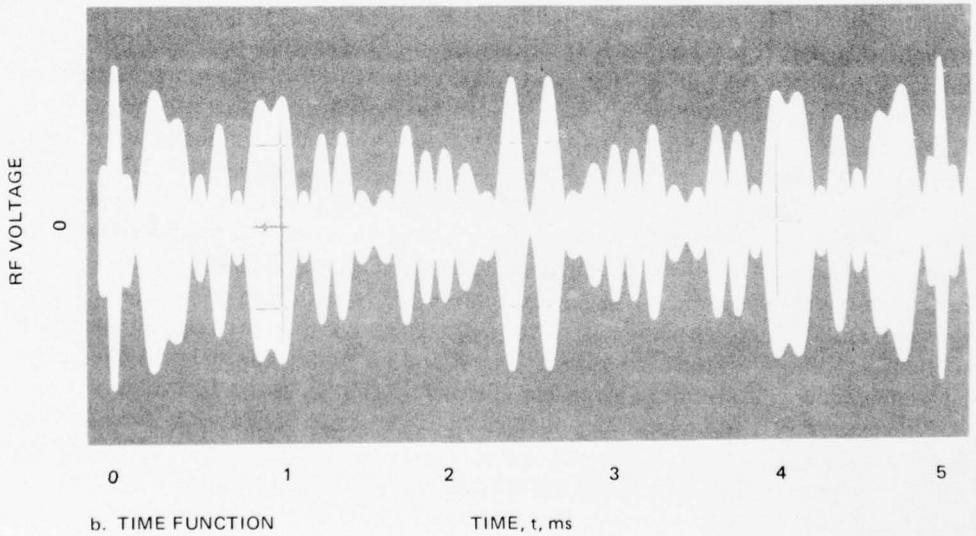

Figure 6. Transmitter output.[3]

changing rapidly. Samples were selected that appeared typical and reasonably stationary. Three of these samples of 10 to 13 minute duration from day and night measurements were analyzed to verify the model. The limiting bandwidths were 12 and 8 kHz on the two daytime samples, 2.5 kHz on the nighttime sample. Since the 11 tones were symmetrically spaced in a 9.6 kHz band about the carrier frequency, it is difficult to interpret the effects of bandwidth beyond 9.6 kHz. Nor are three samples sufficient to state that they are a valid representation of the hf medium. The sunrise/sunset data would have provided valuable data on dispersion if the dispersion alone had been analyzed. Since a sounder was not run coincidentally with the experiment, it was not known how far the observation frequencies were from the operational MUF.

CHANNEL MEASUREMENTS AND THEIR PRACTICAL IMPLEMENTATION

Attention will now be turned to three basic classes of channel measurements which require the use of special purpose equipment.

CLASS 1 CHANNEL MEASUREMENTS

A channel stimulus, x(t), is transmitted repetitively over the hf channel from a base station. Apart from noninterference with other spectrum users, there is no constraint on the form of x(t); it could be a relatively complex coded signal. Specialized processing equipment at a remote station analyzes the received version, y(t), of the channel stimulus and formulates an appropriate path model. In the modeling process, channel estimation data from other sources can be incorporated legitimately if they are appropriate.

The best known implementation of Class I channel measurements is oblique incidence ionospheric sounding, of which several forms are available. The simplest type is a pulse sounder employing time and frequency synchronized transmission and reception. A high-power sounding transmitter radiates short pulses at given times on preset channels that are spaced in frequency over the entire hf band or a part of it. The transmission schedule can be varied as required by a system "program" and is commonly controlled via a clock which can be locked to an external time standard transmission such as WWV. At the remote station, the sounder receiver is synchronized with the same or a similar time transmission. Preferably, for greater time-delay resolution, both transmitting and receiving sites should be equipped with atomic time or frequency standards. When the transmitted pulse x(t) is of short duration, the sounder receiver essentially measures the effective linear unit impulse response function h(t) of that channel. The received signal y(t) is given by the convolution integral:

$$y(t) = \int_{-\infty}^{\infty} h(u)x(t - u)du , \qquad (30)$$

where u is a time variable. If x(t) is an approximate impulse, then y(t) is obviously proportional to the impulse response of the channel. The effect of rapid fluctuations in the mode properties can be reduced if several pulses are transmitted on each frequency and the received responses averaged. Because sounding receivers use narrow pulses, their bandwidths are commonly 30 to 100 kHz; therefore, sounding receivers tend to be more susceptible to interference than normal hf communications equipment.

A most important variant of the basic pulse sounding system is one in which the individual pulses on each frequency are modulated. This confers three important advantages:

1. It allows pulse compression coding to be applied in order to improve the time resolution properties of the system without having to shorten the basic pulse length and hence increase the peak transmitter power.
2. A limited amount of data, such as equipment status, can be transmitted via the pulse modulation coding.
3. It improves performance in high interference environments.

Several forms of pulse compression or pseudorandom codes have been used in practice. These include Barker codes, Huffman sequences, and binary codes (length >13) having approximately aperiodic autocorrelation functions. In all the above cases, impulse responses evaluation is accomplished by computing the input-output cross-correlation function (ccf), $\phi_{xy}(\tau)$, as follows:

$$\phi_{xy}(\tau) = \frac{1}{T} \int_{-T/2}^{T/2} x(t)\, y(t+\tau)dt \tag{31}$$

$$= \int_{-\infty}^{\infty} h(u)\, \phi_{xx}(\tau - u)du\ , \tag{32}$$

where τ and u are time delay variables, T is the correlation interval, and $\phi_{xx}(\tau)$ is the input autocorrelation function. It is seen from equation (32) that if the input aperiodic autocorrelation function is impulsive, then $\phi_{xy}(\tau)$ will be proportional to the system impulse response function.

Coll and Storey[11] describe an application of pulse compression signals to the field of ionospheric sounding. They compare single pulses, binary codes of length 17, and a Huffman impulse-equivalent pulse train of length 17. The basic pulse length used was 25 μs. The energy of the binary code relative to that of a single component pulse with the same peak power was 17 (12.3 dB); its peak-to-maximum-side-lobe ratio was 8.5 to 1 (9.3 dB). The Huffman pulse train has only one component pulse with magnitude of 1 and hence has less energy than the constant magnitude binary signal. The energy of the Huffman signal was 7.28 (8.6 dB) times that of a single pulse of the same peak amplitude; its peak-to-maximum-side-lobe ratio was 10.8 (10.3 dB).

Another variation of the pulse sounder is a new modulation technique based on the use of complementary sequences.[12] If one of the pair of complementary sequences, say

---

[11] DC Coll and JR Storey, Ionospheric Sounding Using Coded Pulse Signal, Radio Science Journal of Research, v 68D, p 1155-1159

[12] M Darnell, Channel Estimation Techniques, paper presented at NATO AGARD Conference Proceedings: Radio Systems and the Ionosphere, Athens, Greece, 26-30 May 1975

$x_1(t)$, is applied to this system, it will give rise to an output $y_1(t)$. Similarly the second sequence $x_2(t)$ will yield an output $y_2(t)$. Employing (32) for each signal in turn:

$$\phi_{x_1y_1}(\tau) = \int_{-\infty}^{\infty} h(u)\, \phi_{x_1x_1}(\tau - u)du \tag{33}$$

and

$$\phi_{x_2y_2}(\tau) = \int_{-\infty}^{\infty} h(u)\, \phi_{x_2x_2}(\tau - u)du\,. \tag{34}$$

Summing (33) and (34),

$$\phi_{x_1y_1}(\tau) + \phi_{x_2y_2}(\tau) = \int_{-\infty}^{\infty} h(u)\left[\phi_{x_1x_1}(\tau - u) + \phi_{x_2x_2}(\tau - u)\right]du\,. \tag{35}$$

Equation (35) shows that the sum of the input-output cross-correlations at equivalent values of τ is equal to the convolution of the system impulse response and the sum of the two individual input autocorrelation functions. This assumes that the two sequences are applied to the linear system in such a way that there are no cross-correlation terms between the two sequences.

In the particular case of ionospheric sounding, there are two ways in which the sequences can be transmitted in order to fulfill this condition. The first, illustrated in figure 7a, is to transmit both simultaneously, in time synchronism, as near to each other in frequency as possible without their spectra overlapping. The respective channel cross-correlation responses could then be summed to give the desired output. A disadvantage of this mode of transmission is that to achieve the required time resolution at the correlation output, the clock rate for the sequences has to be approximately 10 kHz and hence the bandwidth of each sequence would be relatively large. Thus, the frequency separation $(f_A - f_B)$ necessary would be of the order of tens of kHz, which implies that propagation and interference conditions would differ considerably for the two sequences. In the second method, illustrated in figure 7b, the complementary sequences can be transmitted on the same frequency, f_{AB}, sequentially, with sufficient time between them to allow for the decay of all multipath returns due to the first sequence before the second sequence occurs (typically 10 ms). This again means that there is no cross-correlation between the two sequences. In terms of processing this means that the received data corresponding to the first sequence must be stored and correlated in synchronism with the second sequence.[12]

Many individual pulse sounders are in operation all over the world. The US Navy operates the Navy Tactical Sounder System at three transmit sites. France operates an identical transmitter. These transmitters transmit two 13 bit Barker coded sequences 25 ms apart on the same frequency during each sweep. Each of the subpulses is of 200 μs duration. A 13 bit Barker coded pulse increases the received signal-to-noise ratio by 13 (11.1 dB). Hansen and Blitch[13] have shown that the Navy Tactical Sounder receiver has a

---

[13] Naval Electronics Laboratory Center TN 2399, Modifications to the AN/UPR-2 Sounder Receiver, by PM Hansen and JD Blitch, 13 June 1973. Technical Notes are working documents and do not represent an official policy statement of NOSC.

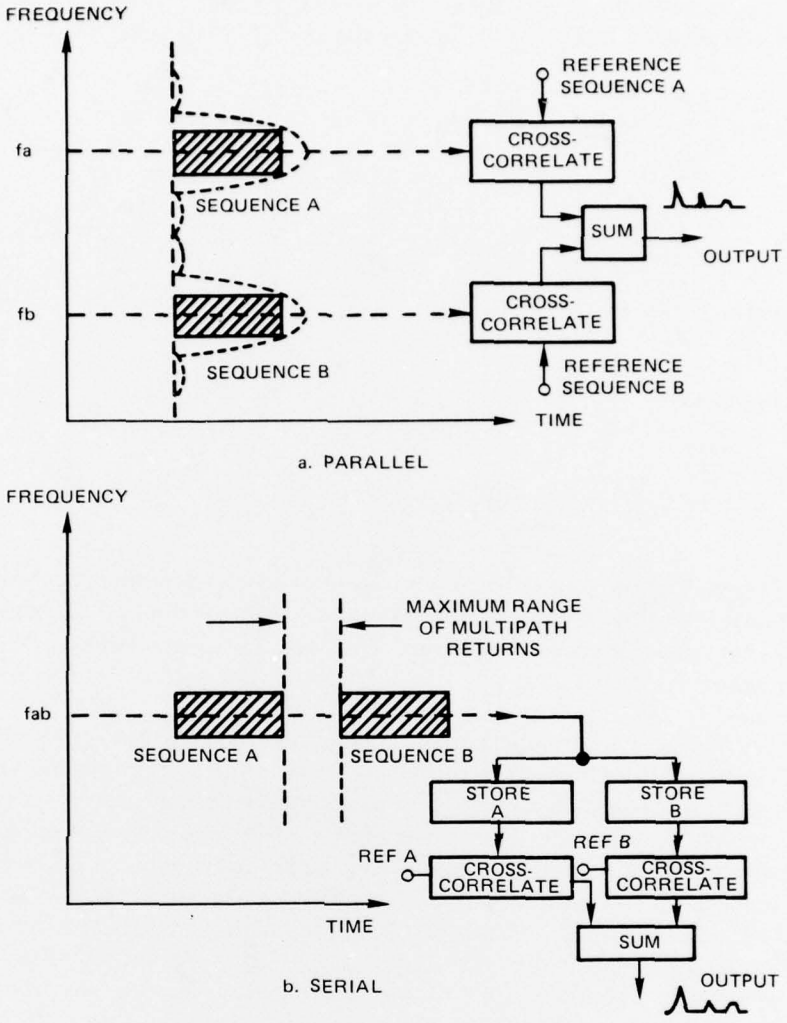

Figure 7. Complementary sequence transmission and processing.[12]

peak-to-maximum-side-lobe ratio of 2 (3dB) without the use of an interference inhibitor circuit and 5 (7.0 dB) with the use of the interference inhibitor. After they modified the test set and realigned the receiver, they obtained a peak-to-maximum-side-lobe ratio of 12 (10.8 dB). They designed a new pulse amplifier for the receiver; its peak-to-maximum-side-lobe ratio was 28 to 1 (14.4 dB).

The only advantage taken of the two sequences in the NTS receiver is in averaging. If a new receiver design were to incorporate a minicomputer or microprocessor, it would be possible to store the first arriving Barker coded pulse and correlate it in synchronism with the second Barker coded pulse. Figure 7b illustrates such a process. This configuration would provide additional processing against impulse noise.

Figure 8 is a functional block diagram of a recommended receiver subsystem. In addition to storing the first transmitted pulse, the microprocessor could be programmed to sense what is happening in the connected receiver and could issue control signals in response to the sensed situation. Hence better accuracy in data collection and a fully documented record of an experiment could be obtained. To insure adequate time delay resolution, the time-frequency standards should be atomic. The terminal is used to control the processor and may be combined with the optional CRT display unit. The go/no-go display is a convenient means of showing ionospheric conditions. The magnetic tape can be used as a permanent record of the experiment. Since it can also be used in the maintenance of the equipment, the mag tape unit should be both a read and write unit. The auxiliary device represents offline equipment not under direct control of the processing unit. This device may be a communication system needing information from the sounding receiver, it may be another computer processor, or it may be a related experiment. For an operating wideband modem, the auxiliary device might provide the necessary frequency dispersion information needed by the modem for its proper operation. The test signal emitted by the sounding receiver is used to calibrate the receiver. (That is, the frequency synthesizer and timing of the frequency sweep in the receiver are utilized by the antenna interface unit to provide the calibration.) The processor controls both the sounding receiver and antenna interface unit.

Another form of ionospheric sounding, fundamentally different in principle from pulse sounding, is "chirp" sounding. Again, a synchronized transmitter and receiver are required; now, however, a low level frequency sweep is transmitted instead of pulses. This sweep can typically be linear or logarithmic in form and can cover part or the whole of the hf band. A replica of the transmitted sweep is generated at the receiver and is used effectively as the local oscillator input. The signal received via the ionospheric path is mixed

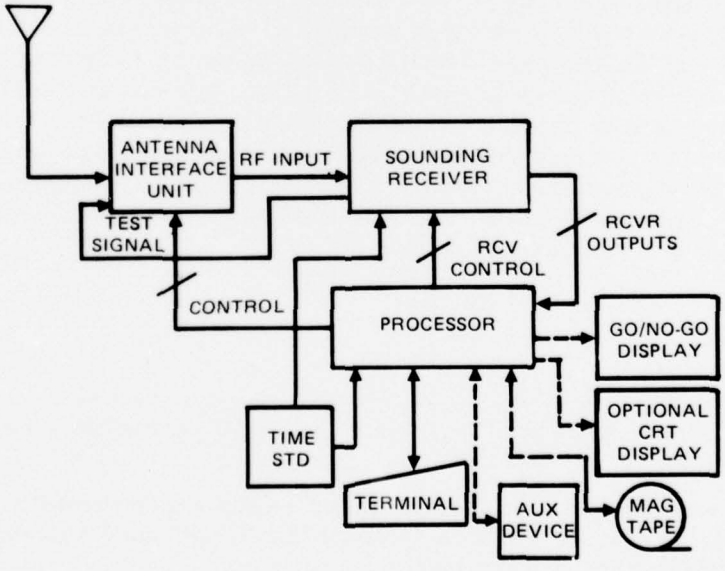

Figure 8. Recommended receiver subsystem functional block diagram.

with this receiver sweep, and the resulting difference signal is subjected to spectrum analysis. Multiple paths give rise to multiple received sweeps with various amplitudes and relative delays. Spectrum analysis shows up the difference frequencies between received sweeps and the local oscillator sweep, with frequency displacement being proportional to the time delay for a linear sweep and amplitudes being correctly translated into the frequency domain.[14] A disadvantage is the confusion of Doppler with time delay.

CLASS 2 CHANNEL MEASUREMENTS

The channel stimulus x(t) is transmitted over the channel, and energy which is reflected back from the channel in the form of a signal y(t) is received at the base and used in the channel estimation processes.

The processing techniques employed in practical Class II systems are, for the most part, very similar to those used in Class I oblique sounders; again they essentially evaluate a linear impulse response function for the channel. However, the fundamental distinction is that the impulse response is measured solely from the base station. Two common forms of single-site sounding exist: vertical incidence sounding and backscatter sounding.

A vertical incidence sounder emits a sounding signal, able to take any of the forms previously described for oblique sounding, which is directed vertically at the ionosphere. The reflected returns are analyzed by a synchronized sounding receiver, and a vertical incidence ionogram is produced. Since transmitter and receiver are now collocated, it is essential that the receiver be desensitized during transmission. The vertical incidence data can be used directly in model formulation for short distance skywave paths; for long range paths, geometrical computations can be applied to the ionogram data to predict oblique incidence properties. Wright has built a prototype digital ionosonde that uses an associated minicomputer and which has very high time delay resolution.[15]

Backscatter sounding is similar to vertical incidence sounding except that the transmitted energy is radiated obliquely instead of vertically. The received signal y(t) is now due to that energy which has propagated via the ionosphere over a path away from the base and has been reflected from the ground back to the base by a similar ionospheric reflection in the reverse sense. Clearly, attenuation in such a system is large and much higher transmitter powers are required; also the definition in the backscatter ionogram is inferior to that in oblique or vertical incidence ionograms. However, backscatter sounding does give a good indication of usable frequency ranges for single-hop paths; the multihop case tends to introduce excessive path loss.

---

[14]GH Barry and RB Fenwick, Extraterrestrial and Ionospheric Sounding with Synthesized Frequency Sweeps, Hewlett-Packard J. v 16, p 8-12, 1965

[15]National Oceanic and Atmospheric Administration ERL SEL Preprint 206, Development of Systems for Remote Sensing of Ionospheric Structure and Dynamics: Functional Characteristics and Applications of the "Dynasonde," by JW Wright, July 1975

CLASS 3 CHANNEL MEASUREMENTS

The channel stimulus x(t) and the base data input b(t) are multiplexed prior to transmission over the hf channel. At the remote station, the received signal y(t) is demultiplexed, processed, and used to formulate a model which then determines the signal processing strategy to be applied to the distorted data signal b'(t) to provide the estimate b(t).

In the pilot tone technique, low level cw tones are either inserted in the data stream or transmitted in potentially available alternate channels. At the receiver, simple phase measurements on the tones enable the relative states of the channels to be specified in terms of predicted data error rates.

TYPES OF SIMULATION EXPERIMENTS

There are several approaches in using a channel simulator to measure the performance capabilities of a modem.[1] On first consideration, the usual thought is to select a set of typical ionospheric channels representing different frequencies in the hf band and different transmitter-to-receiver link distances, time of day, latitude, etc, then to measure the modem performance for each channel. This "typical channel" approach will show the modem's capability for the specific combinations of channel parameters that are selected, and the results can be compared with corresponding measurements on the other modems. It is inefficient, however, because the results usually cannot be used to determine (1) the contribution of each of the types of channel distortion to the modem's degraded performance, (2) the effects of modem-receiver distortions, (3) the manner in which the various distortions combine, or (4) the modem's performance under channel conditions for which measurements have not been made.

In order to utilize channel simulation to its finish, it is necessary to apply some significance to the types of signal distortions caused by the channel. For instance, if it is found that a modem under study has a bit error rate of 10^{-1} for a Doppler frequency shift of 10 Hz, it is necessary to know how and under what circumstances that type of Doppler might occur.

A second approach that could overcome these inefficiencies would be to obtain a complete set of measurements. In the "complete set" approach, a suitable number of numerical values would be used for each channel parameter, and measurements would be made for all combinations of parameter values. By examining selected data subsets in each of which only one distortion parameter changed value, the inefficiencies of the typical-channel approach could be overcome. Unfortunately, the complete-set approach is not practical because of the formidable number of parameter combinations.

A compromise approach that is both efficient and practical might be called the "single and multiple distortions" approach. A channel with only one type of distortion is used first, and a set of measurements of bit and block error probabilities are measured by using successively larger values of the distortion parameter. The set of error probability values obtained in this experiment then defines bit and block error probability curves as functions of the single channel distortion. Similar experiments are performed for other selected channel distortions. The experiments are then expanded to include two types of channel distortion at a time, and error probabilities are measured as functions of one

distortion parameter while the other is held constant. The procedure is continued in selected experiments with three types of channel distortion present, where error probabilities are always measured against one varied channel distortion parameter while the others are held constant. Such performance curves are characterized by from two to five intervals. With decreasing abscissa distortion values, the curves have an upper plateau interval, followed by at least one descending interval, followed in most cases by a second plateau interval, and in some cases by a second descending interval and a third plateau interval. In each interval, one type of channel or modem-receiver distortion usually predominates and the other distortions are relatively insignificant in determining error probabilities. In a small fraction of the intervals, two types of distortion can be comparable and significant. Supplementary measurements of error probabilities versus rms signal level to the modem receiver can be made with constant channel distortion(s), to yield additional information about modem-receiver distortions. When suitable combinations of types of channel distortion are chosen with appropriate parameter values,the various curves are related, and the approach is both efficient and practical. It is efficient because the results can be used to determine the extent to which each type of channel distortion contributes to a modem's degraded performance, the effects of modem-receiver distortions, the manner in which the various distortions combine, and a modem's performance under some channel conditions for which measurements have not been made. The approach is practical because a surprisingly effective set of measurements can be made in a reasonable time. It is the method that was used in the channel-simulator measurements on the USC-10, ACQ-6, and MX-190 modems.[1] The specific types of experiments that were performed are listed in table 2.

TABLE 2. TYPES OF CHANNEL-SIMULATOR EXPERIMENTS.[1]

Nonfading experiments
- Signal level
- Gaussian noise
- Atmospheric noise
- Doppler

Fading experiments
- Fading
- Signal level and fading
- Gaussian noise and fading
- Atmospheric noise and fading
- Cw interference and fading
- Doppler and fading
- Multipath and fading
- Fading and multipath
- Signal level, multipath, and fading
- Gaussian noise, multipath, and fading
- Atmospheric noise, multipath, and fading
- Cw interference, multipath, and fading
- Doppler, Gaussian noise, and fading
- Doppler, multipath, and fading

CONCLUSIONS

An hf channel simulator provides access to the values of parameters of an appropriate real-time ionospheric channel model which describes the path behavior adequately.

While an unproven channel model can provide very useful information, it may not be typical of the hf medium. A desirable mathematically tractable channel model would be one that is known to be a valid representation of the hf medium for the largest practicable percentage of typical hf links.

In general, there are two basic sources of signal distortion associated with hf paths: time dispersion and frequency dispersion. For narrow bandwidths, the ionospheric delay variation is small relative to the multipath spread, and dispersion consequently can be ignored in simulating hf channels. For wide bandwidths, the effect of multiple modes reduces to the production of reverberation. Temporal variations of the ionosphere no longer cause fading, but instead produce only small Doppler shifts (on the order of a fraction of a Hz) between various components of the reverberation. For the wide bandwidths, ionospheric delay variation can cause considerable phase distortion in which the phases of the various frequency components of a signal are altered so that they are not coherently combined by the receiver correlator.

The best known hf channel simulator, developed at ITS by Watterson, is presently capable of accurately simulating all types of channel distortion except manmade noise, for system bandwidths less than 2.5 kHz at night and less than 12 kHz during the day. It is a four-tap delay line. Each tap delivers a delayed but effectively undistorted version of the transmitted signal to a path gain multiplier. Here the signal is modulated in amplitude and phase by an independent, stationary, complex, baseband function termed the path gain function, $G_i(t)$, to provide the frequency-scatter distortion (both Doppler and fading) on that path.

For the analysis of the performance capabilities of modems suffering multiplicative channel distortions, it is useful to have statistical descriptions of the channel frequency-scatter and time-scatter characteristics in addition to the channel-simulator parameters. Watterson derived both channel frequency-scatter and time-scatter characteristic functions in terms of the path gain function $G_i(t)$. The derived functions include channel time-varying frequency response, $H(f, t)$; channel correlation function, $R(\Delta f, \Delta t)$; channel scatter function, $S(\tau, \nu)$; channel frequency scatter function, $V_c(\nu)$; channel attenuation, a_c; channel frequency spread, $2\sigma_c$; channel time-scatter function, $u_c(\tau)$; channel delay, τ_c; and channel time spread, $2\rho_c$.

A source of distortion of ionospherically propagated signals is the dispersion caused by ionospheric refraction. If the phase distortion imposed on a signal is represented by a transfer function of the form $\exp(-i\phi(f))$, the group delay, τ, becomes $d\phi/df$. If τ is not constant, then dispersion, with its consequent distortion, occurs. The dispersion may be regarded as significant if b/2 (half bandwidth) is equal to or greater than $\pi/\sqrt{\Delta\tau/\Delta f}$, where $\Delta\tau/\Delta f$ in s/Hz is the slope on the ionogram at f_o, the center frequency. For a 100 kHz bandwidth, for instance, the dispersion will be significant if $\Delta\tau/\Delta f$ is equal to or greater than 3.14×10^{-4} ms/kHz. The dispersion may be represented by a filter on each tap. It can be approximated by a polynomial function of frequency at a set of orthogonal functions. To measure the dispersion accurately enough to provide the coefficients, the ability to resolve time delay to 62.8 μs, assuming b = 100 kHz, will be necessary. The time frequency scatter functions must be recalculated for each realization of time delay.

In 1969 Watterson reported an experimental verification of his channel model in which a hybrid time-and-frequency domain method was used to obtain propagation measurements. The signal transmitted was amplitude modulated to provide coherent pulses with near-Gaussian envelopes of 50 μs duration at 200 Hz. Superimposed on this pulse were 11 cw tones of equal amplitude. The 11 tones were symmetrically spaced in a 9.6 kHz band. Watterson determined that his model was valid for bandwidths less than 12 kHz during the daytime and 2.5 kHz during the nighttime. The sunrise and sunset data would have provided valuable data on dispersion if the dispersion alone had been analyzed. Furthermore, since his transmitted signal consisted of a 50 μs pulse with 11 cw tones superimposed, his resolution for time delay measurements was 4.5 μs. This resolution is small enough for the necessary dispersion correction filters to be determined.

An alternate approach to hf channel simulation given here is useful whenever the ionospheric dispersion is large enough to cause the Watterson model to require an excessive number of taps. This approach, which uses fast Fourier transform techniques, provides a transfer function for a single propagation mode. The effects of multimoding would have to be handled by a superposition of such transfer functions.

RECOMMENDATIONS

In the development of an hf channel model for the simulation or design of modems, include the effects of both frequency and time dispersion.

To obtain representative channel model data necessary to implement channel simulation, use an oblique sounder system that achieves needed resolution in time delay by employing complementary sequences or modulated pulses.

If the Watterson hf channel simulator is used for frequency bandwidths greater than 2.5 kHz at night and 12 kHz during the day, represent the frequency dispersion by a filter on each tap.

If the spread of arrival times of ionospherically propagated signals would cause an excessive number of taps to be required in the Watterson model, consider the alternate approach of using fast Fourier transforms.

Develop the receiver subsystem described in this report to minimize impulse noise by providing additional processing gain.

To measure the performance capabilities of a modem, use the "single and multiple distortions" approach to channel simulation described in this report.

To determine the time delay versus frequency and range to be inserted in the time delay equation for each mode or propagating path, use the Jones ionospheric ray tracing program.

Generate a report summarizing the channel realization information referenced herein and its relationship to the various ionospheric models in the Jones ray tracing program.

REFERENCES

1. Office of Telecommunications Report 75-56, Hf Channel-Simulator Measurements and Performance Analyses on the USC-10, ACQ-6, and MX-190 PSK Modems, by CC Watterson and CM Minister, July 1975.
2. CC Watterson, JR Juroshek, and WD Bensema, Experimental Confirmation of an Hf Channel Model, IEEE Trans Commun Technol, v 18, p 792 – 803, December 1970.
3. ESSA Technical Report ERL 112-ITS 80, Experimental Verification of an Ionospheric Channel Model, by CC Watterson, JR Juroshek, and WD Bensema, July 1969.
4. ESSA Technical Report ERL 127-ITS 89, Recommended Specifications for Ionospheric Channel and Atmospheric Noise Simulators, by CC Watterson and RM Coon, September 1969.
5. PA Bello, Characterization of Randomly Time-Variant Linear Channels, IEEE Trans Commun Syst, v 11, p 360 – 393, December 1963.
6. Electrophysics Laboratories Project Report 236, Dispersion Correction Study, by RN DeWitt, JR Earhart, and JD Kolesar, August 1973.
7. Electrophysics Laboratories Project Report 243, Dispersion Correction Study, by RN DeWitt, JL Wheeler, and FJ Woods Jr, March 1974.
8. Electrophysics Laboratories Project Report 207, Estimates of Distortion of a Wideband Signal Propagated via the Ionosphere, by RN DeWitt, JR Earhart, and JD Kolesar, September 1972.
9. Office of Telecommunications Report 75-76, A Versatile Three-Dimensional Ray Tracing Computer Program for Radio Waves in the Ionosphere, by RM Jones and JJ Stephenson, October 1975.
10. International Telephone and Telegraph Avionics Division Electro-Physics Laboratories Letter ser no RD-8386, by RN DeWitt, to Naval Electronics Laboratory Center (DB Sailors), Subject: Review of Watterson's IEEE paper, 30 September 1976.
11. DC Coll and JR Storey, Ionospheric Sounding Using Coded Pulse Signals, Radio Science Journal of Research, v 68D, p 1155 – 1159.
12. M Darnel, Channel Estimation Techniques, paper presented at NATO AGARD Conference Proceedings: Radio Systems and the Ionosphere, Athens, Greece, 26 – 30 May 1975.
13. Naval Electronics Laboratory Center TN 2399, Modifications to the AN/UPR-2 Sounder Receiver, by PM Hansen and JD Blitch, 13 June 1973.
14. GH Barry and RB Fenwick, Extraterrestrial and Ionospheric Sounding with Synthesized Frequency Sweeps, Hewlett-Packard J, v 16, p 8 – 12, 1965.
15. National Oceanic and Atmospheric Administration ERL SEL Preprint 206, Development of Systems for Remote Sensing of Ionospheric Structure and Dynamics: Functional Characteristics and Applications of the "Dynasonde," by JW Wright, July 1975.

BIBLIOGRAPHY

NOSC or NELC Technical Notes are working documents and do not represent an official policy statement of NOSC.

WATTERSON MODEL

CC Watterson, JR Juroshek, and WD Bensema, Experimental Confirmation of an Hf Channel Model, IEEE Trans Commun Technol, v 18, p 792 – 803, December 1970.

ESSA Technical Report ERL 112-ITS 80, Experimental Verification of an Ionospheric Channel Model, by CC Watterson, JR Juroshek, and WD Bensema, July 1969.

Office of Telecommunications Report 75-56, Hf Channel-Simulator Measurements and Performance Analyses on the USC-10, ACQ-6, and MX-190 PSK Modems, by CC Watterson and CM Minister, July 1975.

ESSA Technical Report ERL 127-ITS 89, Recommended Specifications for Ionospheric Channel and Atmospheric Noise Simulators, by CC Watterson and RM Coon, September 1969.

ESSA Technical Memorandum ERL TM-ITS 198, An Ionospheric Channel Simulator, by CC Watterson, GG Ax, LJ Demmer, and CH Johnson, September 1969.

ESSA Technical Report ERL 70-ITS 60, Channel Simulation – Digital vs Analog, by EA Quincy, March 1968.

Office of Telecommunications Technical Memorandum 74-177, Simulating Atmospheric Radio Noise at 60 kHz, 200 kHz, and 5 MHz, by EC Bolton, August 1974.

CHANNEL MODELING

PA Bello, Characterization of Randomly Time-Variant Linear Channels, IEEE Trans Commun Syst, v 11, p 360 – 393, December 1963.

Stanford Research Institute Project 4554, research memo 1, Analysis of Multipath Effects on FSK Error Probability for a Simple Hf Channel Model, by RF Daly, July 1964.

Stanford Research Institute Project 4172, Technical Report 2, part 2, On Modeling the Time-Varying Frequency-Selective Radio Channel, by RF Daly, July 1964.

Stanford Research Institute Project 3670, final report, Hf-Communication Effects: Experimental Justification of the Gaussian Channel Model, by BC Tupper and HN Shaver, August 1965.

Stanford Research Institute Project 4554, final report – Phase I, Communication Sounding as an Aid to Frequency Management, by DL Nielson, KD Felperin, DR MacQuivey, and T Kailath, January 1965.

S Stein, Theory of a Tapped Delay Line Fading Simulator, paper presented at IEEE Communications Convention, 1st, Boulder, Colorado, 7 – 9 June 1965.

RA Freudberg, A Laboratory Simulator for Frequency-Selective Fading, paper presented at IEEE Communications Convention, 1st, Boulder, Colorado, 7 – 9 June 1965.

B Goldberg, RL Heyd, and D Pochmerski, Stored Ionosphere, paper presented at IEEE Communications Convention, 1st, Boulder, Colorado, 7 – 9 June 1965.

WE Morrow Jr, Channel Characterization: Basic Approach, Lectures on Communication Systems Theory, ed by EJ Baghdady, 1st ed, p 59 – 69, McGraw-Hill Book Co, Inc, 1961.

H Sherman, Channel Characterization : Rapid Multiplicative Perturbations, Lectures on Communication Systems Theory, ed by EJ Baghdady, 1st ed, p 71 – 94, McGraw-Hill Book Co, Inc, 1961.

T Kailath, Channel Characterization: Time-Variant Dispersive Channels, Lectures on Communication Systems Theory, ed by EJ Baghdady, 1st ed, p 71 – 94, McGraw-Hill Book Co, Inc, 1961.

International Radio Consultative Committee, 13th Plenary Assembly, Geneva, 1974, Report 549; Hf Ionospheric Channel Simulators, Geneva, International Telecommunications Union, 1975.

Stanford Research Institute Project 7161, final report – Phase I, An Experiment to Measure Trans-Atmospheric Wideband Radio Propagation Parameters, EJ Fremouw, September 1969.

Office of Telecommunications Report 76-96, Transmission Channel Characterization by Impulse Response Measurements, by RF Linfield, RW Hubbard, and LE Pratt, August 1976.

Office of Telecommunications Report 75-76, A Versatile Three-Dimensional Ray Tracing Computer Program for Radio Waves in the Ionosphere, by RM Jones and JJ Stephenson, October 1975.

CHANNEL MEASUREMENTS

CC Watterson, JR Juroshek, and WD Bensema, Experimental Confirmation of an Hf Channel Model, IEEE Trans Commun Technol, v 18, p 792 – 803, December 1970.

ESSA Technical Report ERL 112-ITS 80, Experimental Verification of an Ionospheric Channel Model, by CC Watterson, JR Juroshek, and WD Bensema, July 1969.

Stanford Research Institute Project 3670, final report, Hf Communication Effects: Experimental Justification of the Gaussian Channel Model, by BC Tupper and JN Shaver, August 1965.

Stanford Research Institute Project 4554, final report – Phase I, Communication Sounding as an Aid to Frequency Management, by DL Nielson, KD Felperin, DR MacQuivey, and T Kailath, January 1965.

Stanford Research Institute Project 3670, final report, Hf Communication Effects: Phase-Stable Data Reduction Techniques and System Test Results, by RA Shepard, BC Tupper, and JB Lomax, August 1965.

GH Barry, and RB Fenwick, Extraterrestrial and Ionospheric Sounding with Synthesized Frequency Sweeps, Hewlett-Packard J, v 16, p 8 – 12, 1965.

M Darnell, Channel Estimation Techniques, paper presented at NATO AGARD Conference Proceedings: Radio Systems and the Ionosphere, Athens, Greece, 26 – 30 May 1975.

JA Betts, and M Darnell, Real-Time Hf Channel Estimation by Phase Measurements on Low-Level Pilot Tones, paper presented at NATO AGARD Conference Proceedings: Radio Systems and the Ionosphere, Athens, Greece, 26 – 30 May 1975.

Stanford Research Institute Project 7161, final report – Phase I, An Experiment to Measure Trans-Atmospheric Wideband Radio Propagation Parameters, by EJ Fremouw, September 1969.

PA Bello, Measurement of the Complex Time-Frequency Channel Correlation Function, Radio Science, v 68D, p 1161 – 1165, October 1964.

National Oceanic and Atmospheric Administration ERL SEL Preprint 206, Development of Systems for Remote Sensing of Ionospheric Structure and Dynamics: Functional Characteristics and Applications of the "Dynasonde," by JW Wright, July 1975.

Office of Telecommunications Report 76-96, Transmission Channel Characterization by Impulse Response Measurements, by RF Linfield, RW Hubbard, and LE Pratt, August 1976.

DC Coll and JR Storey, Ionospheric Sounding Using Coded Pulse Signals, Radio Science Journal of Research, v 68D, p 1155 – 1159.

R Price, and PE Green Jr, Communication Techniques for Multipath Channels, Proc IRE, v 46, p 555 – 570, 1958.

Naval Electronics Laboratory Center TN 2399, Modifications to the AN/UPR-2 Sounder Receiver, by PM Hansen and JD Blitch, 13 June 1973.

CHANNEL REALIZATION

Office of Telecommunications Report 75-56, Hf Channel-Simulator Measurements and Performance Analyses on the USC-10, ACQ-6, and MX-190 PSK Modems, by CC Watterson and CM Minister, July 1975.

ESSA Technical Report ERL 127-ITS 89, Recommended Specifications for Ionospheric Channel and Atmospheric Noise Simulators, by CC Watterson and RM Coon, September 1969.

Office of Telecommunications Technical Memorandum 74-177, Simulating Atmospheric Radio Noise at 60 kHz, 200 kHz and 5 MHz, by EC Bolton, August 1974.

International Radio Consultative Committee, 13th Plenary Assembly, Geneva, 1974 Report 549; Hf Ionospheric Channel Simulators, Geneva International Telecommunication Union, 1975.

Southwest Research Institute Task Report XXXIII, Contract N00039-72-C-1275, Measured Sea Path Skywave/Groundwave Signal Power Ratios Over the 2-10 MHz Range, by JE Hipp and TC Green 23 January 1976.

Stanford Research Institute Project 3670, final report, Hf Communication Effects: Frequency Dispersion and Doppler Shift, by RA Shepherd, August 1965.

Stanford Research Institute Project 3670, final report, Hf Communication Effects: Propagation in the High-Latitude Ionosphere, by TI Dayharsh et al, August 1965.

Stanford Research Institute Project 3670, final report, Hf Communication Effects: Executive Summary, by JB Lomax, August 1965.

Stanford Research Institute, Contract DA-36-039SC-87197, DASA 1739, Hf DATA Compendium: Power Spectra and Oblique Ionograms, by RA Shepherd, BC Tupper, and JB Lomax, July 1965.

Stanford Research Institute, Contract DA-36-039SC-87197, DASA 1740, Hf Data Compendium: Phase, by RA Shepard, BC Tupper, and JB Lomax, July 1965.

Stanford Research Institute, Contract DA-36-039SC-87197, DASA 1740, Hf DATA Compendium: Amplitude, by RA Shepherd, BC Tupper, and JB Lomax, July 1965.

Electrophysics Laboratories Project Report 293, Coastal Surveillance with OTH Radar: Feasibility Test Results, by JL Wheeler and HG Tornatore, June 1976.

Electrophysics Laboratories Project Report 175, Measured Attenuation of Hf Groundwaves, by JL Wheeler, December 1970.

JL Wheeler, A Review of the Experiment to Characterize Surface-Wave Propagation Over the Seawater at Radio Frequencies, Stanford Research Institute Project 2304, Proceedings of the Teal Wing Conference – Summer 1975, v 2, June 1975.

L Bede and A Peled, A New Hardware Realization of High-Speed Fast Fourier Transforms, IEEE Transactions on Acoustic, Speech, and Signal Processing, v ASSP-23, no 6, p 543 – 547, 1975.

CHANNEL MODELING FOR WIDE BANDWIDTHS

Electrophysics Laboratories Project Report 236, Dispersion Correction Study, by RN DeWitt, JR Earhart, and JD Kolesar, August 1973.

Electrophysics Laboratories Project Report 243, Dispersion Correction Study, by RN DeWitt, JL Wheeler, and FJ Woods Jr, March 1974.

Electrophysics Laboratories Project Report 207, Estimates of Distortion of a Wideband Signal Propagated via the Ionosphere, by RN DeWitt, JR Earhart, and JD Kolesar, September 1972.

JL Wheeler, A Review of the Experiment to Characterize Surface-Wave Propagation Over the Seawater at Radio Frequencies, Stanford Research Institute Project 2304, Proceedings of the Teal Wing Conference – Summer 1975, v 2, June 1975.

DJ Belknop, RD Haggarty, and BD Perry, An Adaptive Signal Processing for Ionospheric Distortion Correction, OHD Technical Review Meeting of 23 – 25 October 1968, v 2, October 1968.

TN DeWitt, JR Earhart, and JD Kolesar, The Effects of Ionospheric Dispersion for Wideband Signals, OHD Technical Review Meeting of 3 – 4 May 1972, Stanford Research Institute, SRI 2-4657, May 1972.

ESSA Research Laboratories Technical Memorandum ERL TM-ITS 188, Advantages of Wideband Modulation in Short Mf-Hf Communication Links, by CC Watterson, July 1969.

International Telephone and Telegraph Avionics Division Electro-Physics Laboratories Letter serial no RD-8386 by RN DeWitt, to Naval Electronics Laboratory Center (DB Sailors), Subject: Review of Watterson's IEEE Paper, 30 September 1976.

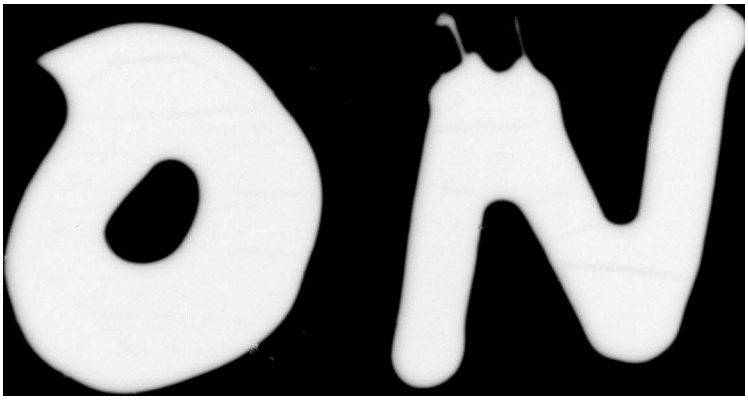
ON

AD-A043 384 NAVAL OCEAN SYSTEMS CENTER SAN DIEGO CALIF F/G 17/2.1
SIMULATION AND MEASUREMENT OF HIGH FREQUENCY IONOSPHERIC CHANNE--ETC(U)
APR 77 D B SAILORS, J R HILL

UNCLASSIFIED NOSC/TR-111 NL

2 OF 2
AD
A043384

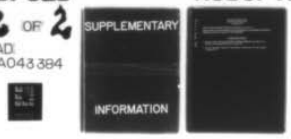

END
DATE
FILMED
1 -78
DDC

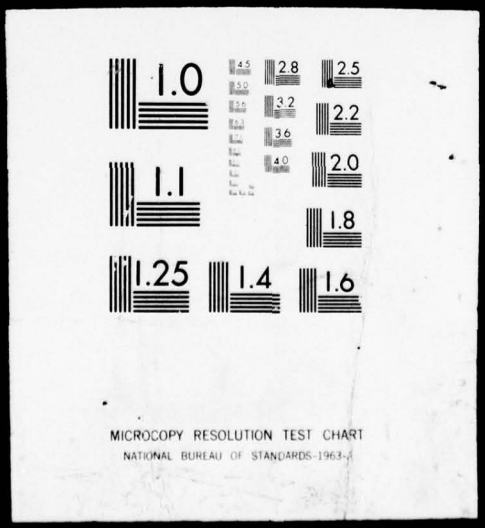

SUPPLEMENTARY

INFORMATION

Naval Ocean Systems Center
San Diego, California 92152
17 August 1977

NAVAL OCEAN SYSTEMS CENTER Technical Report 111 (TR 111)

SIMULATION AND MEASUREMENT OF HIGH FREQUENCY IONOSPHERIC CHANNELS, DB Sailors and JR Hill, 22 April 1977, UNCLASSIFIED

LITERATURE CHANGE

1. On cover, under NAVAL ELECTRONIC SYSTEMS COMMAND, and in Block 11 of DD Form 1473, change PME 107-031 to ELEX 310.

2. On cover, after date 22 April 1977, and in Block 12 of DD Form 1473, add "changed 17 August 1977"